ACS Macro Letters

Letter

pubs.acs.org/macroletters

Tube Curvature Slows the Motion of Rod–Coil Block Copolymers through Activated Reptation

Muzhou Wang,[†] Alexei E. Likhtman,[‡] and Bradley D. Olsen*[,†]

[†]Department of Chemical Engineering, Massachusetts Institute of Technology, Cambridge, Massachusetts 02139, United States

[‡]School of Mathematical and Physical Sciences, University of Reading, Reading RG6 6AX, U.K.

Supporting Information

ABSTRACT: Understanding the dynamics of molecules with complex shapes is important as researchers develop advanced materials using hybrid molecules. This study applies a slip-spring model to visualize and quantify the entangled dynamics of rod–coil block copolymers. The parameters of the model are determined by matching with molecular dynamics simulation results. By monitoring the positions of polymers along the entanglement tube, rod–coil copolymers are shown to disfavor configurations where the rod occupies curved portions of the tube of randomly varying curvature created by the coil ends. This confirms that reptation of copolymers occurs by an activated mechanism and is the first demonstration of the activation barriers that have been previously inferred through diffusion measurements by simulation and experiment. The barriers to diffusion are further quantified by considering the curvilinear motion of ring polymers, and their effect on diffusion is quantitatively captured by considering one-dimensional motion along an entanglement tube with a rough free energy potential.

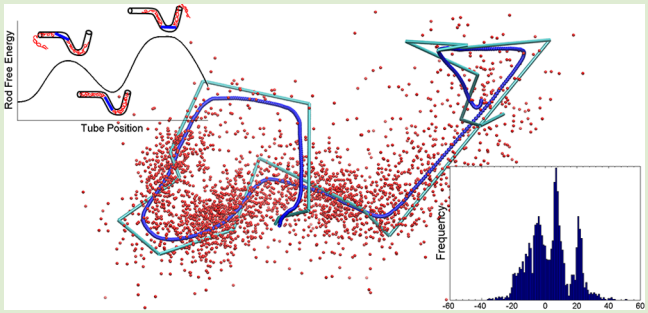

Soft matter and polymer physics have devoted increasing attention to self-assembled systems composed of complex shapes.[1,2] Individual domains are combined into hybrid molecules and shape amphiphiles,[3,4] with each motif contributing a different functionality such as electronic properties[5,6] or biological activity.[7,8] While the thermodynamics of distinct molecular shapes introduce many interesting phenomena such as packing entropy[9] and liquid crystalline interactions,[10] dynamic effects are also important for predicting material flow properties, designing manufacturing processes,[11] and understanding the new physics that directly arises from the motion of connected domains of dissimilar geometries.

Rod–coil block copolymers are an example of hybrid molecules that have attracted recent interest for organic electronics[6] and biomaterials.[8] For entangled homopolymers, reptation theories and experimental measurements have shown divergent scaling behaviors between rods (isotropic self-diffusion $D \sim M^{-1}$, longest relaxation time $\tau_r \sim M^{9}$)[12−14] and coils ($D \sim M^{-2.3}$, $\tau_r \sim M^{3.4}$)[13,15−17] due to the geometrical differences between rigid rods and Gaussian coils. Recently, we proposed a reptation theory of entangled rod–coil copolymers, with dual relaxation mechanisms arising from the mismatch between the curvatures of the entanglement tubes of the rod and coil blocks.[18−20] In the small rod limit where the rod is a perturbation on coil motion, the randomly varying curvature of the coil's tube presents entropic barriers to the reptation of the rod, modifying the unhindered motion of the coil along its tube into an activated reptation process. In the large rod limit where the coil is a perturbation on rod motion, the long rod cannot rotate around the surrounding entanglements so motion is only possible when the coil moves into a straightened entanglement tube in an arm retraction process. These mechanisms are supported by Kremer-Grest molecular dynamics (MD) simulations and experimental diffusion measurements using forced Rayleigh scattering.[18−20]

This letter presents a detailed analysis of the activated reptation mechanism using a new coarse-grained slip-spring model to demonstrate and quantify the random entropic barriers to rod reptation in the small rod limit. This analysis of activated reptation is distinct from previous studies which inferred the mechanism through simulation and experimental diffusion measurements and is an important component in the overall theory of entangled rod–coil dynamics. Our model simulates highly entangled rod–coil systems by expanding upon existing slip-spring models that have successfully reproduced entanglement dynamics in coil homopolymers.[21] First, the slip-spring model is quantitatively matched with previous Kremer-Grest simulation results for tracer diffusion of coil–rod–coil triblock copolymers in high molecular weight coil homopolymers. The barriers in the activated reptation mechanism are then observed by simulating symmetric copolymers over a large time window before end effects, arm

Received: November 19, 2014
Accepted: January 21, 2015
Published: January 29, 2015

DOI: 10.1021/mz5007377
ACS Macro Lett. 2015, 4, 242−246

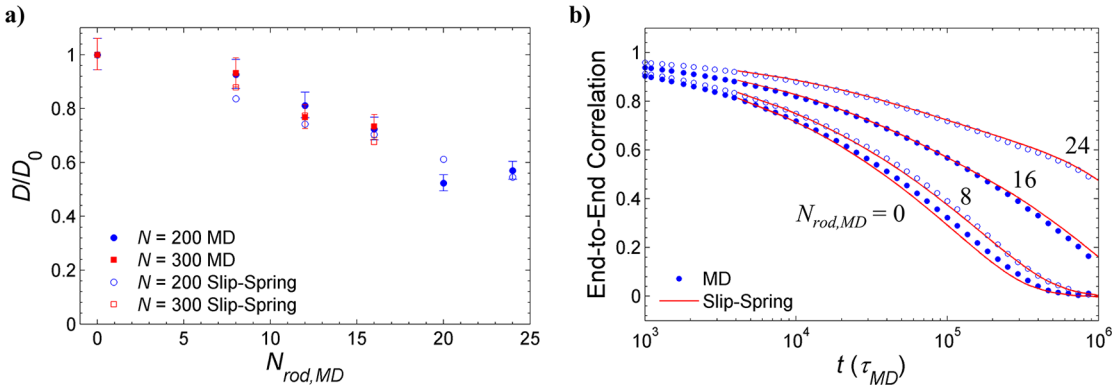

Figure 1. (a) Normalized center-of-mass diffusion of coil−rod−coil triblocks of a given total size for both MD simulation and the slip-spring model. MD diffusivities are calculated over 760 chains,[18] and slip-spring data are calculated over 2400 chains. (b) End-to-end relaxation functions of triblocks with N = 200 are compared between MD (blue dots) and slip-spring (red lines) for $N_{rod,MD}$ = 0, 8, 16, and 24.

retractions, and tube reorganization events become important. Finally, the size of these barriers is quantified by simulation of ring polymers, and their effect on diffusion is captured by a simple analytical model of one-dimensional motion along a nonuniform free energy potential.

The current work simulates symmetric coil−rod−coil triblocks with N = 800 monomers at low rod fractions in the absence of constraint release using a modification of Likhtman's single-chain slip-spring model.[21] This regime has been explored experimentally[19] and corresponds to well-entangled rod−coil systems with high coil fractions. Furthermore, the large coil blocks isolate the effects of activated reptation by minimizing arm retraction events. In this model, coil blocks consist of Rouse chains connected to the end of a rigid thin rod block, with entanglements simulated by slip-springs that connect fixed anchor points $\mathbf{a}_j$ with Hookean springs to slip-links $\mathbf{s}_j$ that reside on monomers. The total energy for a chain of N monomers is given by

$$U = \frac{3k_BT}{2b^2}\sum_i (\mathbf{r}_{i+1} - \mathbf{r}_i)^2 + \frac{3k_BT}{2N_sb^2}\sum_{j=1}^{Z}(\mathbf{a}_j - \mathbf{s}_j)^2 \quad (1)$$

where $\mathbf{r}_i$ are the positions of the coil monomers and the rod ends; b is the coil statistical segment length; N_sb^2 is the mean-square extension of a slip-spring; and $Z = N/N_e$ is the number of slip-springs per chain, with N_e as the average number of monomers between slip-links. Chains are simulated using Brownian dynamics with a coil monomer friction ζ. b serves as the characteristic unit length, and the unit time is $\tau = \zeta b^2/(k_BT)$. To simulate reptation, the slip-links move between adjacent monomers by a Monte Carlo scheme, where each slip-link undergoes a trial move of one monomer every 0.002τ with a Metropolis acceptance criterion. Two slip-links are not allowed to move onto the same monomer, so entanglements cannot cross. At least 10 polymers are simulated simultaneously, and slip-links moving off a chain end are destroyed and then created at the end of a randomly selected chain.

Although the slip-spring model is a coarse-grained single-chain model,[22] careful selection of the model parameters leads to quantitative matching of observables between slip-spring and MD simulations.[23,24] The end-to-end distance of MD coil polymers is $\langle R^2\rangle = 1.32^2N_{coil}\sigma_{MD}^2$ for the length unit σ_{MD}, so the scale factor between length units is $b = 1.32\sigma_{MD}$. By comparing monomer mean-square displacement and end-to-end relaxation (Supporting Information), good agreement between MD and slip-spring coil homopolymers is observed with N_e = 35, N_s = 5, and a scale factor between time units of $\tau_{SL} = 41\tau_{MD}$. These parameters are consistent with previous matching studies on similar models,[23,24] as well as previously observed entanglement spacings[25] and tube radii.[25,26]

To simulate rod−coil block copolymers, the slip-spring model must first be extended to rod-like polymers and validated using Kremer-Grest simulations for rod homopolymers. In contrast to MD rods which were represented by monomers with a stiff three-bead bending potential,[18] rod blocks in the slip-spring model are perfectly rigid and thus fully determined by a position, orientation, and length L_{rod}. The dynamics are governed by an anisotropic mobility tensor, with a parallel friction of $\zeta_\parallel = (1.23\zeta L_{rod}/b)/\log(2.20L_{rod}/b)$, perpendicular friction of $\zeta_\perp = \zeta_\parallel/6$, and rotational friction of $\zeta_{rot} = (L_{rod}/b)^{3.92}/26.9$, determined by comparing anisotropic mean-square displacement and rotational correlation functions with MD simulations (Supporting Information). The functional form of the translational friction is that of a dilute rod,[13] while an empirical power law was used for rotation. To allow the motion of slip-links, the rigid rod was discretized into a series of monomers of size b_{rod}, such that the length $L_{rod} = N_{rod}b_{rod}$ matches the MD length $L_{rod} = N_{rod,MD}\sigma_{MD}$. Entanglements move along these rod monomers in the same way as coil monomers with N_e = 35 and N_s = 5, so the selection of b_{rod} determines the slip-link density along the rod, with average length between entanglements of $L_{e,rod} = N_eb_{rod}$. In this study, the rod slip-link density was set at $b_{rod} = \sigma_{MD}/4 = b/1.32/4$ and $N_{rod} = 4N_{rod,MD}$. To maintain the MD convention, we will denote $N_{rod,eff} = N_{rod,MD} = N_{rod}/4$ and total number of monomers as $N = N_{coil} + N_{rod,eff}$.

The key parameters determined from separately matching coil and rod homopolymer are $b = 1.32\sigma_{MD}$, $\tau_{SL} = 41\tau_{MD}$, $N_{e,coil}$ = 35, $L_{e,rod} = 35b/1.32/4 = 6.63b$, and N_s = 5. While these parameters were determined by comparing dynamic properties, they also automatically result in similar distributions of slip-spring anchor points around rods and coils (Figure S4 in Supporting Information). This is consistent with both blocks diffusing through the same matrix, specifically an entangled coil homopolymer matrix. Most importantly, slip-spring simulation of coil−rod−coil triblock copolymers quantitatively reproduces diffusion and end-to-end relaxation dynamics observed in MD simulations of the same triblocks (Figure 1a,b), without any changes to the parameters determined from matching

DOI: 10.1021/mz5007377
ACS Macro Lett. 2015, 4, 242−246

homopolymer dynamics. This validates the application of the slip-spring model to studies of rod−coil copolymers.

The slip-spring model has many significant advantages over explicit MD simulation. Because there are no excluded volume interactions and the surrounding matrix is not simulated, computational speedups of many orders of magnitude over MD are achievable. While moderately entangled $N = 300$ chains were barely feasible in MD, $N = 800$ chains corresponding to $Z > 22$ entanglements are easily accessible in the slip-spring model. This is particularly important for observing activated reptation, where large coil blocks minimize changes to the tube shape from the rod and arm retraction events. Entanglements are explicitly defined in the slip-spring model, so observation of 1D motion along the tube is straightforward and avoids challenges in defining the tube in MD.[25,27−31] The slip-spring tube can be defined by connecting the anchor points, and the 1D position of the polymer is found by projecting the center monomer onto the line segment connecting the two nearest slip-spring anchor points.

Using these advantages of the slip-spring model, direct observation of the activated reptation mechanism is possible (Figure 2a). Ten $N = 800$ chains with $N_{rod,eff} = 0$ or 12 in the middle (coil homopolymer or coil−rod−coil) are equilibrated for $(2 \times 10^6)\tau$, which is significantly longer than the coil reptation time of $\tau_{rep} \approx (4.2 \times 10^5)\tau$. 2880 independent simulations with different random seeds are then initialized from the same configurations for each chain, and the 1D positions of the rod along the tube are calculated at every time point. These positions are valid until the rod moves into tube segments that have been renewed from the ends since initialization. As time increases, the distribution of 1D positions spreads from an initial delta function at $t = 0$. For a coil homopolymer, this distribution evolves as a Gaussian 1D diffusion process, which is expected as motion parallel to the tube should be unhindered (Figure 2b). For a block copolymer, the 1D positions spread nonuniformly, with rod locations in straight segments of the 3D tube favored and locations in highly curved segments disfavored (Figure 2c). As predicted by activated reptation, this effect arises because there are fewer available configurations for both the rod and the surrounding entangling chains when the rod is in a curved tube section. The results here confirm that rod−coils diffuse along an underlying free energy surface of the tube that is nonuniform, providing direct evidence for the activated reptation mechanism.

While the coil−rod−coil triblocks provide an excellent demonstration of hindered diffusion due to activated reptation, quantification of the underlying free energy surface is difficult because the phenomenon can only be transiently observed due to continuous tube renewal from the chain ends. This renewal due to reptation and contour length fluctuation processes prevents measurement of the equilibrium ensemble of tube positions. As an example, the polymers in Figure 2b are shown after $\sim 0.12\tau_{rep}$ and thus have not explored the extent of the tube, but ~1% of the ensemble has already moved into renewed tube segments.

The challenges in quantifying free energy are overcome by using rod−coil rings rather than linear coil−rod−coil triblocks. Replacement with rings is commonly used to better understand the entanglement behavior of linear polymers.[25,30,32] Because ring entanglements are permanent in the absence of constraint release, statistics can be collected indefinitely without considering disengagement phenomena. Twenty rod−coil rings were equilibrated as described in the Supporting

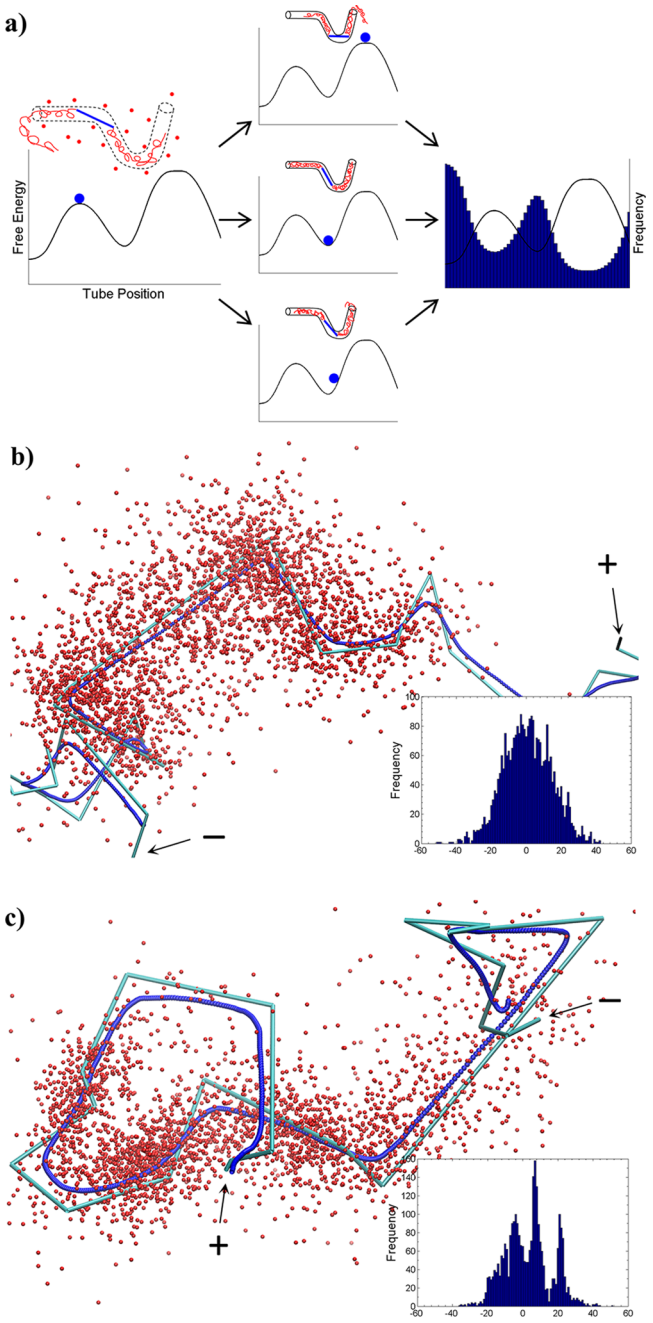

Figure 2. (a) Nonuniform free energy potential in the activated reptation mechanism can be observed by initializing many independent simulations from a single configuration. The position of the polymers along the tube (blue dot on free energy diagram) is then tracked over time and compiled into a frequency distribution that reflects the underlying potential. 2880 chains of $N = 800$ were initialized from a well-equilibrated configuration of a (b) coil homopolymer and (c) symmetric coil−rod−coil triblock copolymer of $N_{rod,eff} = 12$. The ensemble of polymers diffuses along the tube, and the positions of the center monomers (red) are shown after $(5 \times 10^4)\tau$. The tube defined by connecting the anchor points (cyan) or Likhtman's tube axis algorithm[25] (blue) are shown. The insets show histograms of 1D tube positions with positive and negative directions indicated in the tube visualizations.

Information, and 600 independent trajectories were initialized from these configurations. After $10^6\tau$ or $\sim 2.4\tau_{rep}$ of exploration in the fixed entanglements, 1D tube positions of the rod center

DOI: 10.1021/mz5007377
ACS Macro Lett. 2015, 4, 242−246

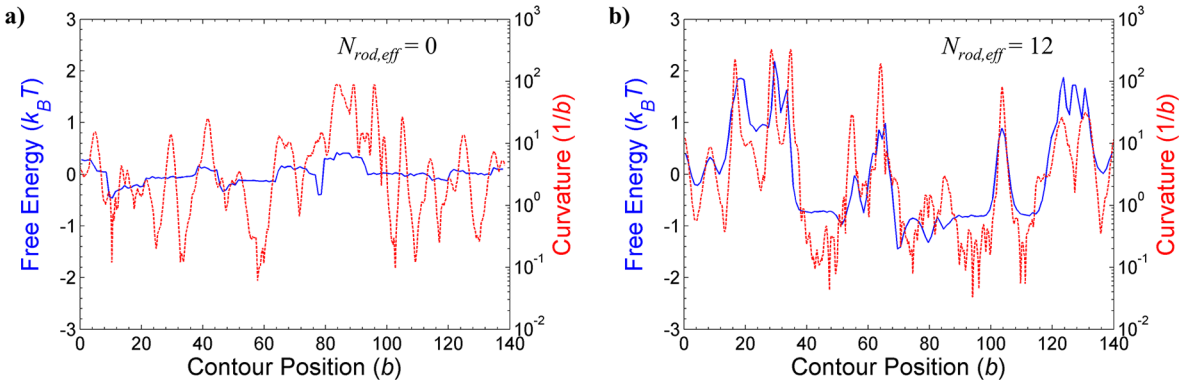

Figure 3. Free energy (blue solid) of the polymer as a function of position s along the tube defined by connected anchor points is plotted with the curvature (red dotted) of the tube axis for randomly chosen rings of N = 800 monomers as (a) coil homopolymers and (b) rod−coils with $N_{rod,eff}$ = 12. The free energies were determined within at most $\pm 0.2 k_BT$ with 95% confidence (details in Supporting Information).

were calculated and collected every $10^3\tau$ over a timespan of $(1.4 \times 10^6)\tau$ into a probability distribution $P(s)$ as a function of the contour position along the connected anchors, s (Figure S8 in Supporting Information). The resulting distributions were not sensitive to the exploration time. The free energy was derived then from the Boltzmann relation, $F(s) = -k_BT \log P(s)$.

The resulting free energies are significantly more nonuniform for rod−coils than coil homopolymers. While fluctuations less than k_BT in the coil homopolymer free energy arise from the tube positioning algorithm and the intrinsic variability of the tube (Figure 3a), the free energy with $N_{rod,eff}$ = 12 has many barriers over $3k_BT$ (Figure 3b). To further explore the physics underlying activated reptation, the curvature of the tube was calculated to compare with the variations in free energy. Because the tube defined by connecting adjacent anchor points is piecewise linear with no defined curvature, a smooth tube was generated using Likthman's tube axis algorithm,[25] which defines the tube as an average of chain conformations over time. The curvature of this tube axis was then mapped onto the previously calculated 1D tube positions (details in the Supporting Information). For the rod−coil, the large free energy variations match very well with the calculated curvature (Figure 3b), confirming that areas of the tube with high curvature have high free energy. The curvature−energy matching can be shown for many rod lengths (Figure S10 in Supporting Information), and the characteristic size of the free energy barriers increases with rod length as predicted by the activated reptation mechanism.

The nonuniform free energy of rod−coils presents significant barriers to curvilinear diffusion along the tube. The effect on diffusion can be estimated by treating the polymer as a single particle exploring the potential. Using Zwanzig's formulation based on a mean first-passage time calculation,[33] a particle with 1D diffusivity D_{c0} moving along a perfectly smooth potential with additional roughness $F(s)$ (Figure 3b) has a diffusivity

$$D_c = \frac{D_{c0}}{\langle e^{-F/k_BT}\rangle\langle e^{F/k_BT}\rangle} = \frac{D_{c0}L_c^2}{\int_0^{L_c} e^{-F(s)/k_BT}\,ds \int_0^{L_c} e^{F(s)/k_BT}\,ds} \quad (2)$$

where L_c is sufficiently large to capture the free energy variations, taken here as the length of the ring tube. Diffusion of rod−coil rings with varying rod length was calculated using eq 2 for all 20 potentials at each condition (Figure 4). Because the characteristic roughness of the potential increases with rod length, the diffusivity decreases as expected for activated

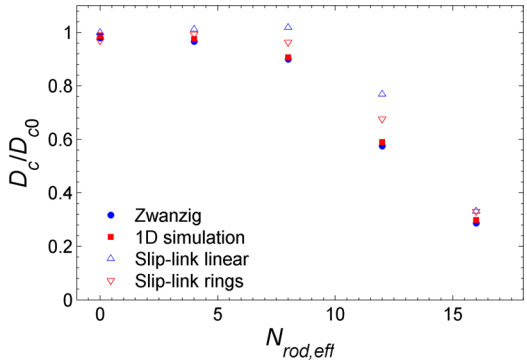

Figure 4. Curvilinear diffusion along the tube as a function of rod length, comparing results from analyzing the 1D free energy potentials with direct measurements from the slip-spring simulation for linear and ring rod−coil polymers. The normalization D_{c0} is the diffusivity of a free particle for the 1D analysis and a linear coil homopolymer for the slip-spring simulations.

reptation. To confirm the prediction of eq 2, simple Brownian dynamics simulations were performed on each potential, and the resulting diffusivities match quite well. For comparison, the curvilinear diffusion of 2400 linear and ring rod−coils of the same size and rod length was measured directly from the slip-spring model by computing the mean-squared displacement of 1D positions along the tube. The linear and ring curvilinear diffusion agree well with each other, suggesting that rings are a good model for rod−coils in this limit.

The agreement between the predictions of the nonuniform potential analysis and the curvilinear diffusion results from the slip-spring model is excellent. Both models predict a factor of 3 change in diffusivity at the largest rod length of $N_{rod,eff}$ = 16, suggesting that the rough free energy potential provides a valid mechanism for the slowed diffusion observed in the slip-spring model. The nonuniform potential analysis slightly underpredicts diffusion in the slip-spring simulations at the intermediate rod lengths of $N_{rod,eff}$ = 8 and 12 because 3-dimensional degrees of freedom that potentially provide accelerated pathways for reptation are averaged out in the 1D analysis. This discrepancy is reduced for the longer rod lengths as these degrees of freedom are diminished with more entanglements on the rod. Nevertheless, the calculated free energy potentials capture the overall diffusion behavior and provide a quantitative understanding of the activated reptation mechanism.

DOI: 10.1021/mz5007377
ACS Macro Lett. 2015, 4, 242−246

In summary, this study highlights the nonintuitive dynamic processes that arise inherently from combining domains of dissimilar shapes within the same molecule. For rod−coil copolymers, varying stiffness along the polymer yields slowed dynamics because reptation proceeds along a rough potential. The resulting activation barriers occur because of the mismatch between the rod and the randomly varying curvature of the entanglement tube. By extending the slip-spring model to rod polymers and block copolymers, the barrier heights were quantified, and the effect on diffusion was shown to follow 1D motion in a rough potential. The dramatically slowed dynamics of rod−coils observed here, in MD simulation, and measured by experiments has important implications for technological applications that require self-assembly and processing of these materials. These results also suggest that shape amphiphiles can demonstrate not only rich thermodynamics but also complex and nonintuitive dynamic phenomena.

■ ASSOCIATED CONTENT

Supporting Information

Further discussion of matching molecular dynamics and slip-spring simulations, additional tube statistics, polymer distributions, curvatures, and free energies of linear and ring polymers. This material is available free of charge via the Internet at http://pubs.acs.org.

■ AUTHOR INFORMATION

Corresponding Author

*E-mail: bdolsen@mit.edu.

Author Contributions

The manuscript was written through contributions of all authors. All authors have given approval to the final version of the manuscript.

Notes

The authors declare no competing financial interest.

■ ACKNOWLEDGMENTS

We gratefully acknowledge funding from NSF Award CMMI-1246740. Simulations were performed on the Kraken and Darter clusters at the NICS and the Gordon cluster at the SDSC through a generous XSEDE allocation TG-DMR110092. Some graphics were generated using Visual Molecular Dynamics.[34] M.W. acknowledges support through NDSEG and NSF Graduate Research Fellowships. A.E.L. acknowledges funding from EPSRC Award EP/K017683.

■ REFERENCES

(1) Glotzer, S. C.; Solomon, M. J. *Nat. Mater.* **2007**, *6* (8), 557−562.
(2) Sacanna, S.; Korpics, M.; Rodriguez, K.; Colon-Melendez, L.; Kim, S. H.; Pine, D. J.; Yi, G. R. *Nat. Commun.* **2013**, DOI: 10.1038/ncomms2694.
(3) Zhang, W. B.; Yu, X. F.; Wang, C. L.; Sun, H. J.; Hsieh, I. F.; Li, Y. W.; Dong, X. H.; Yue, K.; Van Horn, R.; Cheng, S. Z. D. *Macromolecules* **2014**, *47* (4), 1221−1239.
(4) Olsen, B. D.; Shah, M.; Ganesan, V.; Segalman, R. A. *Macromolecules* **2008**, *41* (18), 6809−6817.
(5) Hadziioannou, G. *MRS Bull.* **2002**, *27* (6), 456−460.
(6) Segalman, R. A.; McCulloch, B.; Kirmayer, S.; Urban, J. J. *Macromolecules* **2009**, *42* (23), 9205−9216.
(7) Klok, H. A. *J. Polym. Sci., Part A: Polym. Chem.* **2005**, *43* (1), 1−17.
(8) van Hest, J. C. M. *Polym. Rev.* **2007**, *47* (1), 63−92.
(9) Damasceno, P. F.; Engel, M.; Glotzer, S. C. *Science* **2012**, *337* (6093), 453−457.
(10) Olsen, B. D.; Segalman, R. A. *Mater. Sci. Eng. R* **2008**, *62* (2), 37−66.
(11) Thomas, C. S.; Xu, L. Z.; Olsen, B. D. *Biomacromolecules* **2012**, *13* (9), 2781−2792.
(12) Doi, M.; Edwards, S. F. *J. Chem. Soc., Faraday Trans. II* **1978**, *74*, 560−570.
(13) Doi, M.; Edwards, S. F. *The Theory of Polymer Dynamics*; Clarendon: Oxford, 1986.
(14) Tracy, M. A.; Pecora, R. *Annu. Rev. Phys. Chem.* **1992**, *43*, 525−557.
(15) Tao, H.; Lodge, T. P.; von Meerwall, E. D. *Macromolecules* **2000**, *33* (5), 1747−1758.
(16) McLeish, T. C. B. *Adv. Phys.* **2002**, *51* (6), 1379−1527.
(17) Lodge, T. P. *Phys. Rev. Lett.* **1999**, *83* (16), 3218−3221.
(18) Wang, M.; Alexander-Katz, A.; Olsen, B. D. *ACS Macro Lett.* **2012**, *1* (6), 676−680.
(19) Wang, M.; Timachova, K.; Olsen, B. D. *Macromolecules* **2013**, *46* (4), 1651−1658.
(20) Wang, M.; Timachova, K.; Olsen, B. D. *Macromolecules* **2013**, *46* (14), 5694−5701.
(21) Likhtman, A. E. *Macromolecules* **2005**, *38* (14), 6128−6139.
(22) Kremer, K.; Grest, G. S. *J. Chem. Phys.* **1990**, *92* (8), 5057−5086.
(23) Sukumaran, S. K.; Likhtman, A. E. *Macromolecules* **2009**, *42* (12), 4300−4309.
(24) Ramirez, J.; Sukumaran, S. K.; Likhtman, A. E. *Macromol. Symp.* **2007**, *252*, 119−129.
(25) Likhtman, A. E. *Soft Matter* **2014**, *10* (12), 1895−1904.
(26) Zhou, Q.; Larson, R. G. *Macromolecules* **2006**, *39* (19), 6737−6743.
(27) Everaers, R.; Sukumaran, S. K.; Grest, G. S.; Svaneborg, C.; Sivasubramanian, A.; Kremer, K. *Science* **2004**, *303* (5659), 823−826.
(28) Foteinopoulou, K.; Karayiannis, N. C.; Mavrantzas, V. G.; Kroger, M. *Macromolecules* **2006**, *39* (12), 4207−4216.
(29) Zhou, Q.; Larson, R. G. *Macromolecules* **2005**, *38* (13), 5761−5765.
(30) Bisbee, W.; Qin, J.; Milner, S. T. *Macromolecules* **2011**, *44* (22), 8972−8980.
(31) Read, D. J.; Jagannathan, K.; Likhtman, A. E. *Macromolecules* **2008**, *41* (18), 6843−6853.
(32) Qin, J.; Milner, S. T. *Soft Matter* **2011**, *7* (22), 10676−10693.
(33) Zwanzig, R. *Proc. Natl. Acad. Sci. U.S.A.* **1988**, *85* (7), 2029−2030.
(34) Humphrey, W.; Dalke, A.; Schulten, K. *J. Mol. Graphics* **1996**, *14*, 33−38.

DOI: 10.1021/mz5007377
ACS Macro Lett. 2015, 4, 242−246